Pressure-induced luminescence of cerium-doped gadolinium gallium garnet crystal

A. Kaminska,[1,*] A. Duzynska,[1] M. Berkowski,[1] S. Trushkin,[1] and A. Suchocki[1,2]
[1]*Institute of Physics, Polish Academy of Sciences, Al. Lotników 32/46, 02-668 Warsaw, Poland*
[2]*Institute of Physics, Kazimierz Wielki University, Weyssenhoffa 11, Bydgoszcz 85-072, Poland*
(Received 30 September 2011; revised manuscript received 22 March 2012; published 6 April 2012)

Studies of the spectroscopic properties of Ce^{3+} dopant in bulk $Gd_3Ga_5O_{12}$:Ce crystal under pressure are presented. In spite of strong intershell $4f \rightarrow 5d$ absorption bands at ambient pressure, the cerium luminescence in $Gd_3Ga_5O_{12}$ is entirely quenched even at low temperature. It has been shown that applying pressure allows for recovery of the $5d \rightarrow 4f$ radiative transitions. Further increase of pressure improves the emission efficiency. This effect is analyzed in terms of two possible phenomena: (i) by pressure-induced electronic crossover of the excited $5d$ energy level of the Ce^{3+} with the conduction band bottom of the host crystal, and (ii) by decrease of electron-lattice coupling with increasing pressure, resulting in reduction of the Stokes shift and nonradiative transitions between the low vibrational levels of the $5d$ state and high vibrational levels of the ground $4f$ state. The results of high-pressure absorption and luminescence measurements point out that the ambient-pressure luminescence quenching is caused by the donor-like charge transfer processes due to the resonant location of the Ce^{3+} $5d$ electronic levels with respect to the host conduction band. In such a situation, the ionization of Ce^{3+} to Ce^{4+} occurs, accompanied by large lattice relaxation, which enables the nonradiative recombination to the Ce $4f$ state. The pressure-induced approach of the conduction-band bottom of the host crystal by the excited $5d$ energy level of the Ce^{3+} results in mixing between conduction band states and the $5d$ state, and the broadband luminescence from this mixed state is observed at pressures from 30 up to about 60 kbar. Then, for pressures exceeding 60 kbar, this luminescence is replaced by the classic Ce^{3+} $5d \rightarrow 4f$ transitions. Using a simple anticrossing model and configuration coordinate model in the appropriate pressure range, quantitative description of the system has been carried out, and the pressure-induced decrease of electron-lattice coupling has been shown.

DOI: 10.1103/PhysRevB.85.155111 PACS number(s): 07.35.+k, 71.70.Ch, 78.40.−q, 78.55.−m

I. INTRODUCTION

Cerium-doped materials are the subject of numerous studies as solid state laser materials,[1,2] phosphors,[3–8] and scintillators.[9,10] Ce^{3+} has the simplest $4f^n$ configuration ($n = 1$), and its broadband emission originating from parity-allowed interconfigurational $4f^0 5d^1 \rightarrow 4f^1 5d^0$ transitions is also studied from the point of view of further understanding of $d \rightarrow f$ luminescence processes, both experimentally[11–13] and theoretically.[14–16]

In different host crystals, Ce^{3+} ions generally show an emission in the near-UV–blue spectral range, but in the presence of strong crystal fields, such as in garnets, visible emissions up to red color are observed.[3–18] However, in some gallium-substituted garnets, like $Y_3Ga_5O_{12}$:Ce and $Gd_3Ga_5O_{12}$:Ce, the luminescence is entirely quenched even at low temperatures.[17–20] This effect has been analyzed in detail by Hansel *et al.* in $Y_3(Al_{1-x}Ga_x)_5O_{12}$:Ce ($0 \leqslant x \leqslant 0.75$) and has been ascribed to the presence of strong electron-lattice coupling and the small splitting of the $5d$ sublevels in the garnets with more cubic structure, which increased the probability of nonradiative transitions from the excited state to high vibrational levels of the ground state.[20] Actually, the structure of $Gd_3Ga_5O_{12}$ garnet (GGG) is expected to be more cubic than, for instance, the structure of $Y_3Al_5O_{12}$ (YAG), in which the cube-like surroundings of dodecahedrally coordinated cations is highly compressed by a tetragonal distortion.[6–21] Then taking into account that, in garnets, rare earth ions substitute dodecahedral sites with D_2 point group symmetry,[22] where the excited $5d$ state splits into five sublevels, and comparing the values of noncubic crystal field splitting parameter δ_1, defined as the energy difference between the two lowest sublevels of the $5d$ level, the higher values of this parameter are observed in garnets with strong Ce^{3+} photoluminescence (PL; about 7470 cm^{-1} in $Y_3Al_5O_{12}$:Ce[11,18] and about 7200 cm^{-1} in $Gd_3Sc_2Al_3O_{12}$:Ce),[23] whereas lower values are found in garnets in which Ce^{3+} PL is completely quenched (about 4300 cm^{-1} in $Y_3Ga_5O_{12}$:Ce[11] and about 5200 cm^{-1} in $Gd_3Ga_5O_{12}$:Ce, this work—see Fig. 1 and the text in the Sec. III A).

The quenching of the Ce^{3+} luminescence has been observed also in a number of nongarnet oxide hosts, like La_2O_3:Ce, La_2O_2S:Ce, Y_2O_3:Ce, and Lu_2O_3:Ce.[24–26] In all these cases, on the base of optical and photoconductive spectroscopic measurements, the authors ascribed the effect to the resonant location of $5d$ cerium levels with respect to conduction band (CB) of the host, which occurs when the host band gap is equal or smaller than 45 000 cm^{-1} (about 5.6 eV).[25] In such a situation, the excited electron relaxes to the bottom of the CB, which is located below the lowest cerium $5d$ level. Thus, the electron does not return to this level, but relaxes in a nonradiative decay processes to the Ce^{3+} ground state, causing the quenching of the luminescence. Such a conclusion was confirmed by Shen *et al.*,[27] who obtained the Ce^{3+} luminescence by applying pressure to the nonemitting Lu_2O_3:Ce system, which induced electronic crossover of the excited $5d$ state of the Ce^{3+} with the CB edge of Lu_2O_3.

Despite the efforts in explaining mechanisms that govern the great differences in luminescence efficiency of Ce^{3+}-doped materials,[20–29] the understanding of this problem is still not complete. By using pressure, we reduce the ion-ion distances

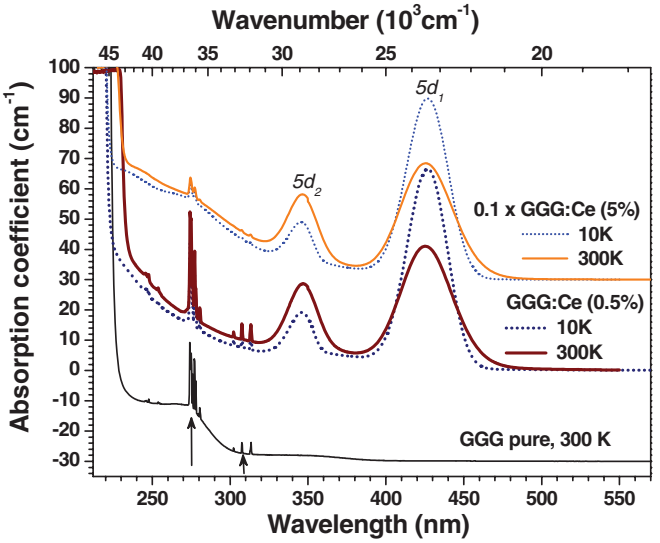

FIG. 1. (Color online) Ambient pressure absorption spectra of pure GGG, GGG:Ce (0.5%), and GGG:Ce (5%) crystals. The spectra of pure GGG and GGG:Ce (5%) are shifted for clarity along the vertical axis by $+20$ cm^{-1} and -20 cm^{-1}, respectively. Additionally, the spectrum of GGG:Ce (5%) is divided by 10. Arrows indicate the gadolinium absorption lines.

in the compressed material, and in this way—both inducing changes of energy bands of host crystal and increasing considerably the crystal field strength experienced by the dopant ion—the high pressure spectroscopy is very well suited for studying such systems. High-pressure spectroscopy was previously used for studying properties of GGG:Mn,[30] GGG:Yb,[31] and GGG:Nd crystals,[32] and several others, for example, lanthanum lutetium gallium garnet ($La_3Lu_2Ga_3O_{12}$, LLGG) doped with chromium and neodymium,[33] and lithium niobate ($LiNbO_3$, LN) doped with Cr[34] or Yb.[35]

In this paper, we describe the effect of pressure on the optical properties of bulk GGG:Ce crystal, which belongs to the nonemitting materials at ambient pressure. At about 30 kbar, we observe the appearance of Ce^{3+}-related PL and then the pronounced increase in the PL intensity with increasing pressure. To analyze this effect, apart from pressure PL measurements, we performed also the measurements of absorption under pressure, which allowed for direct determination of pressure dependence of the Stokes shift. Our results reveal that the ambient pressure luminescence quenching is caused by the resonant location of the Ce^{3+} $5d$ electronic levels in the host conduction band, similar to the case of Lu_2O_3:Ce.[27] When the Ce^{3+} $5d$ electronic levels are resonant with the CB, efficient photoionization of Ce^{3+} and electron delocalization occurs, followed by nonradiative decay of excited electrons due to strong host lattice relaxation around the Ce^{4+} ion. The pressure-induced crossover of the conduction-band bottom of the host crystal with the first excited $5d$ energy level of the Ce^{3+} ion (denoted further as $5d_1$) results in strong mixing of $5d_1$ and CB states and the appearance of the relatively broad and initially weak luminescence associated with the radiative recombination of the mixed state at pressures between 30 and 60 kbar. Because most likely the delocalized electron remains in the vicinity of ionized Ce^{4+} ion due to its attractive Coulomb potential, the observed luminescence can be associated with the formation of Ce-trapped exciton (CTE), i.e. the bound electron-hole pair with the hole localized on the cerium impurity and the electron on a nearby lattice site. Such an impurity-trapped luminescence, called the anomalous luminescence, was observed and analyzed in Ce^{3+}-doped Cs_3LuCl_6 (Ref. 36) and elpasolite Cs_2LiYCl_6 and $Cs_2LiLuCl_6$ crystals,[37,38] as well as in Yb^{2+}-doped[39–41] and Eu^{2+}-doped[41–46] crystals.

Finally, at pressures exceeding 60 kbar, when the minimum of the emitting $5d_1$ state of Ce^{3+} shifts below the conduction band edge, the conventional highly efficient $4f^0 5d \rightarrow 4f^1$ emission of Ce^{3+} is observed. Theoretical analysis of experimental data using the single configuration coordinate model of the system allowed us to obtain good agreement between the model and experiment.

The paper is organized as follows: in Sec. II, we describe the investigated samples and the experimental methods. In Sec. III, the results of spectroscopic studies of the GGG:Ce crystal (absorption and luminescence) are reported. In Sec. IV, we present the quantitative analysis of experimental data based on the configuration coordinate diagram of the system and anticrossing model and discuss all obtained results. Finally, a summary and conclusions are presented in Sec. V.

II. SAMPLES AND EXPERIMENTAL TECHNIQUES

Two GGG:Ce samples were grown by the Czochralski method. The concentration of Ce^{3+} ions in the sample used for PL measurements was equal to 0.5 at.%, whereas the concentration of Ce^{3+} ions in the sample used for high-pressure absorption measurements was equal to 5 at.%. The sample with lower Ce^{3+} concentration was grown to avoid the presence of luminescence lines originating from Ce-Ce pairs. However, because of a small amount of Ce^{3+} dopant in the GGG:Ce(0.5%) sample and very low thickness of the sample that can be loaded into the diamond anvil cell (DAC), the cerium absorption of this sample was not detectable under pressure. Therefore, the GGG:Ce(5%) sample was grown specially for high-pressure absorption measurements.

Trying to obtain the ambient pressure photoluminescence, we used several available laser lines of the continuous wave (cw) Coherent Innova 400 Ar-ion laser working in the wavelength range from deep-UV (275.4 nm), through near-UV (between 333.6 and 363.8 nm), up to visible (457.9 nm), as well as the 405-nm line of the GaN semiconductor laser (OEM laser product). High-pressure PL spectra were measured, finally, using a 457.9-nm line of the Coherent Innova 400 Ar-ion laser as the main excitation source; however, in several complementary measurements, three other Ar-laser lines from the visible spectral region (476.5, 488, and 496.5 nm) have also been used. The spectra were dispersed by a Horiba Jobin-Yvon FHR 1000 monochromator. The signal was detected by means of a liquid nitrogen cooled charge-coupled device (CCD) camera. The high-pressure measurements were performed using a low-temperature diamond anvil cell (CryoDAC LT, easyLab Technologies Ltd). Argon was used as a pressure-transmitting medium. The DAC was mounted in an Oxford Optistat CF cryostat equipped with a temperature controller for low-temperature measurements. The samples, cut and

polished down to a thickness of 20 μm, were loaded into the cell along with a small ruby crystal. The R_1-line ruby luminescence was used for pressure calibration.[47–49] The line width of ruby luminescence was also used for monitoring hydrostatic conditions in the DAC.[50,51]

The ambient-pressure absorption spectra were measured with a Cary 5000 UV-Vis-NIR spectrophotometer. The high-pressure absorption measurements were performed in the DAC using a double gasket as the sample chamber. The sample covering the smaller hole into the rear thin gasket was illuminated via an optical fiber coupled to an Ocean Optics DH2000 Deuterium Tungsten Source. The spectra of transmitted light were measured with the use of a Horiba Jobin-Yvon FHR 1000 monochromator in the same configuration as in the case of measuring of emission spectra. Absorbance of the sample was determined using a standard formula, i.e. as a logarithm of the relative intensity of light transmitted by DAC with an empty gasket and DAC loaded with the sample.

III. EXPERIMENTAL RESULTS

A. Absorption spectra of pure GGG, GGG:Ce(0.5%), and GGG:Ce(5%) crystals at ambient pressure

The ambient pressure room-temperature (RT) absorption spectra of pure GGG, GGG:Ce(0.5%), and GGG:Ce(5%) crystals are presented in Fig. 1. Additionally, the absorption spectra of GGG:Ce(0.5%) and GGG:Ce(5%) samples measured at 10 K are presented for comparison. The measurement of pure GGG allowed for determination of the energy gap of the host crystal, which occurred to be equal to 5.57 eV at 10 K and 5.33 eV at RT, revealing slight temperature energy gap shrinkage.

There are visible two absorption bands originating from $4f^15d^0 \rightarrow 4f^05d^1$ transitions of the Ce^{3+} ions, denoted as $5d_1$ and $5d_2$. In the distorted cubic site occupied by Ce^{3+} ions (D_2 point group symmetry), $4f$ ground electronic configuration splits into two states $^2F_{5/2}$ and $^2F_{7/2}$. This splitting in garnets is in the range of 2000 cm^{-1},[6] and in absorption, the transitions from the ground $^2F_{5/2}$ state are observed. The excited $5d$ configuration is split in this symmetry into five sublevels: lower doublet and higher triplet.[11] The results show that the energies of $^2F_{5/2} \rightarrow 5d_1$ and $^2F_{5/2} \rightarrow 5d_2$ transitions, peaked at about 426 nm (23 500 cm^{-1}) and 348 nm (28 700 cm^{-1}), respectively, are smaller than the band-gap energy of the host crystal; whereas the energies of higher-lying $5d_3$, $5d_4$, and $5d_5$ levels are greater than the band-gap energy of the host crystal; so they are not visible in the absorption spectra. However, the measured spectra do not allow us to resolve unambiguously, whether the $5d_1$ and $5d_2$ states are located in the energy gap or are resonant with the conduction band of the host, as the transitions from the Ce^{3+} ground state $^2F_{5/2}$ to the CB states are much less probable than the intraconfigurational $^2F_{5/2} \rightarrow 5d$ transitions of Ce^{3+} ion.

The extent of the tetragonal distortion from perfect cubic structure is described by the total crystal field splitting parameter, defined as the energy difference between the highest and the lowest level of the split $5d$ state.[11,52] However, in many compounds, similar to the case of GGG, the higher sublevels are not visible; therefore, the distortion is often described by the crystal field splitting δ_1 parameter, defined as the energy difference between the two lowest sublevels of the $5d$ state.[6] This parameter can be determined for GGG:Ce directly from the measured absorption spectra: it is equal to (5200 $\pm$ 200) cm^{-1} and does not depend on cerium concentration. This relatively small value as compared to other garnets[11,18,23] indicates low distortion of Ce^{3+} surrounding from cubic symmetry in GGG.

B. Pressure dependence of the luminescence of Ce^{3+} ions in GGG crystal at low temperature

Despite the observed strong absorption of Ce^{3+} in GGG, no luminescence was observed either under direct continuous wave (cw) excitation into cerium absorption bands [with six available Ar-ion laser lines between 333.6 and 363.8 nm, or the 405-nm line of GaN semiconductor laser (OEM laser product)], or through exciting the gadolinium with the 275.4-nm line of an argon ion laser.

After the application of pressure to this nonemitting system, at about 30 kbar, weak broad luminescence in the spectral range between 10 400 cm^{-1} (960 nm) and 20 400 cm^{-1} (490 nm) appeared, under the excitation with a 457.9-nm line of an argon ion laser. Further increasing the pressure caused pronounced increase in PL intensity, accompanied by the initial decrease of the width of the emission band at the pressures from 30 kbar up to 60 kbar. This last effect will be discussed in more detail in Sec. III D.

The PL spectra of Ce^{3+} in GGG at $T = 10$ K as a function of hydrostatic pressure, in the pressure range up to about 194 kbar, are shown in Fig. 2. The spectra consist of two overlapping broad bands, corresponding to two transitions from the lowest sublevel of the excited $5d$ state to the $^2F_{7/2}$ (lower energy band, peak labeled as #1) and $^2F_{5/2}$ (higher energy band, peak labeled as #2) sublevels of the $4f$ ground state. The broad appearance of these bands is a consequence of strong coupling of the excited $5d$ state to the surrounding lattice.[15,29,53,54] The strong sharp emission features round 14 000 cm^{-1} are due to the ruby pressure calibrant used in the experiment, which is located in a DAC chamber next to the sample, and its luminescence is so strong that it is unavoidable in such an experiment.

The PL spectra have been deconvoluted into two Gaussian bands, and in this way, the pressure dependence of the spectral positions of the two components as well as their intensities have been obtained. The results are presented in Fig. 3. The spectral positions of the GGG:Ce luminescence lines depend nonmonotonically on pressure. The energies of the peaks initially increase, and after reaching maxima at about 60–65 kbar, they decrease with increasing pressure. This behavior is unusual, as with increasing pressure, we rather expect the decrease of transition energies due to the increase in the $5d$ state splitting and as a result decrease of the energy of the lowest $5d_1$ sublevel.[55–58] In comparison with the $5d$ state, the pressure shift of the $4f$ state energies can be neglected, as the inner-shell $4f$ electrons are well shielded from the lattice by the $5s$ and $5p$ electrons; and therefore, their energies are not significantly affected by the pressure induced crystal field changes,[31,35,59–61] as it is in the case of the much less-screened outer $5d$ state.

The PL intensity of the GGG:Ce increases strongly with increasing pressure up to about 100 kbar, and for pressure

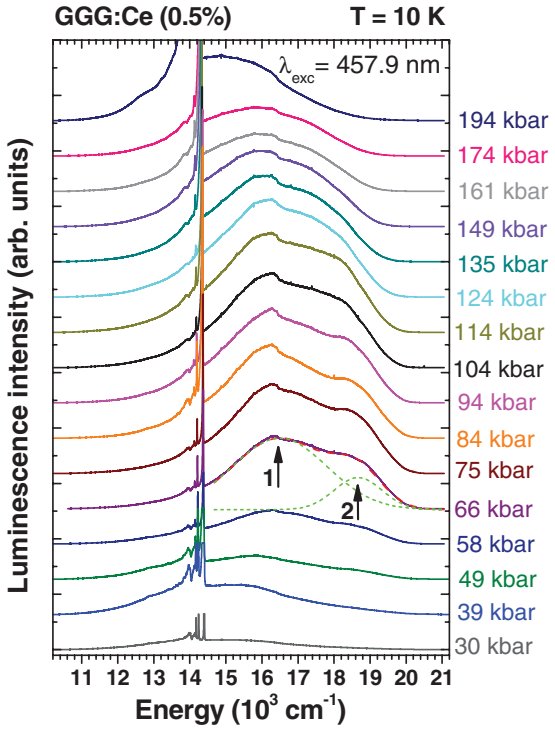

FIG. 2. (Color online) The pressure dependence of the PL spectra of Ce^{3+} in GGG crystal. The emission features round 14 000 cm^{-1} are due to the ruby pressure calibrant used in the experiment. Arrows indicate transitions from the lowest sublevel of the $5d$ state to the (1) $^2F_{7/2}$ and (2) $^2F_{5/2}$ sublevels of the $4f$ ground state. An example of fitted curves is presented on the spectrum at the pressure of 66 kbar.

exceeding 120 kbar, gradual decrease in PL intensity is observed. We attribute this effect to a red shift of the $5d_1$ excitation band of Ce^{3+}, causing the reduction in excitation efficiency and decrease of PL intensity. Indeed, the change of excitation to longer wavelengths with increasing pressure allowed for intensity recovery, which is shown in Fig. 4.

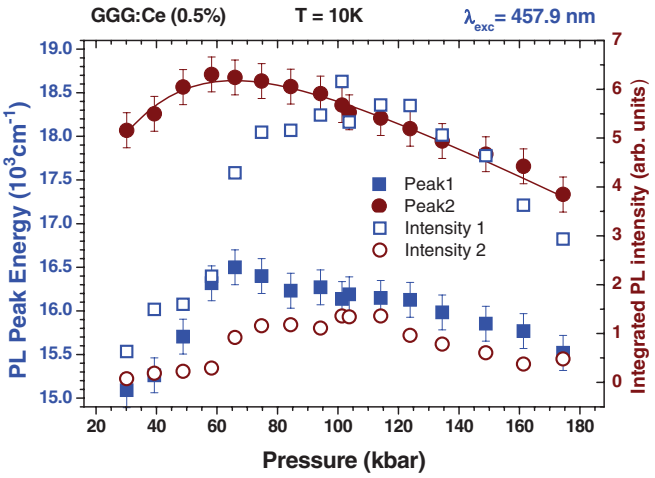

FIG. 3. (Color online) The pressure dependence of the PL peak energies and integrated PL peak intensities of GGG:Ce crystal. The solid line represents the best fit of the model to the experimental data (see the description in Sec. IV B).

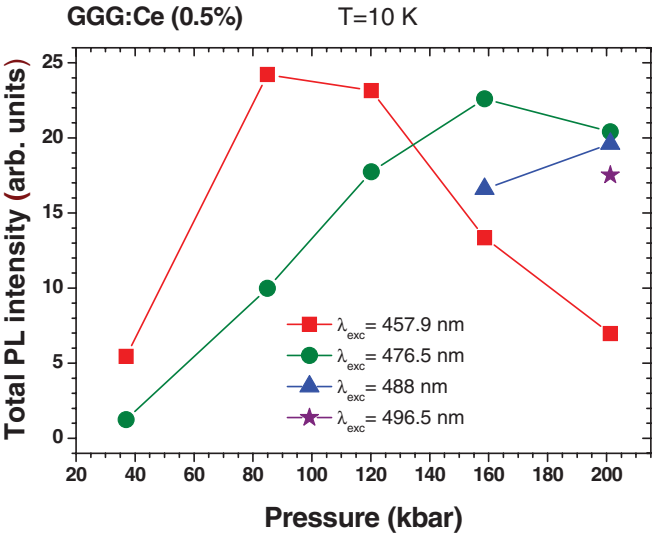

FIG. 4. (Color online) The pressure dependence of the total PL intensity excited with different argon laser lines. Changes in the excitation efficiency reflect pressure red shift of the excited $5d_1$ level. Lines connecting the measurement points are only guides for eyes.

C. Pressure dependence of the absorption spectra of Ce^{3+} ions in GGG crystal at room temperature

The absorption spectra of GGG:Ce have been measured in the pressure range from 0 up to 105 kbar. As it has been already mentioned in Sec. II, because of a small amount of Ce^{3+} dopant and a very low thickness of the sample that can be loaded into the DAC, the cerium absorption was not detectable in the GGG:Ce(0.5%) sample. For this reason, the high-pressure absorption measurements have been performed on the GGG:Ce(5%) sample. Comparing the ambient-pressure absorption spectra of both samples (see Fig. 1), which differ only in the values of absorption coefficients and have the same energy positions of the absorption lines originating from $4f^15d^0 \rightarrow 4f^05d^1$ Ce^{3+} transitions as well as the line widths, we assume that results obtained for these samples can be used for generalized analysis of the pressure behavior of cerium dopant in GGG.

The pressure dependence of the absorption spectra of Ce^{3+} ions in GGG measured at RT is presented in Fig. 5. Unlike in the case of luminescence, both absorption lines show the noticeable continuous decrease of peak energies with increasing pressure. Up to the highest measured pressure, the two lowest absorption lines of $^2F_{5/2} \rightarrow 5d_1$ transitions of the Ce^{3+} ions are visible.

From the measured absorption spectra, we can determine both the pressure dependence of absorption energies and the pressure dependence of the δ_1 parameter, which allows us to monitor the pressure changes of the distortion of the Ce^{3+} ion surrounding from perfect cubic structure. The absorption peak energies of Ce^{3+} ions in GGG and the crystal field splitting parameter δ_1 as a function of pressure are presented in Fig. 6. If we approximate the pressure dependence of absorption peak energies and the δ_1 parameter by linear fits, we obtain the pressure coefficients as slopes of these fits equal to (-21 ± 1) cm^{-1}/kbar for the $^2F_{5/2} \rightarrow 5d_1$ transition, (-20 ± 1) cm^1/kbar for the $^2F_{5/2} \rightarrow 5d_2$ transition,

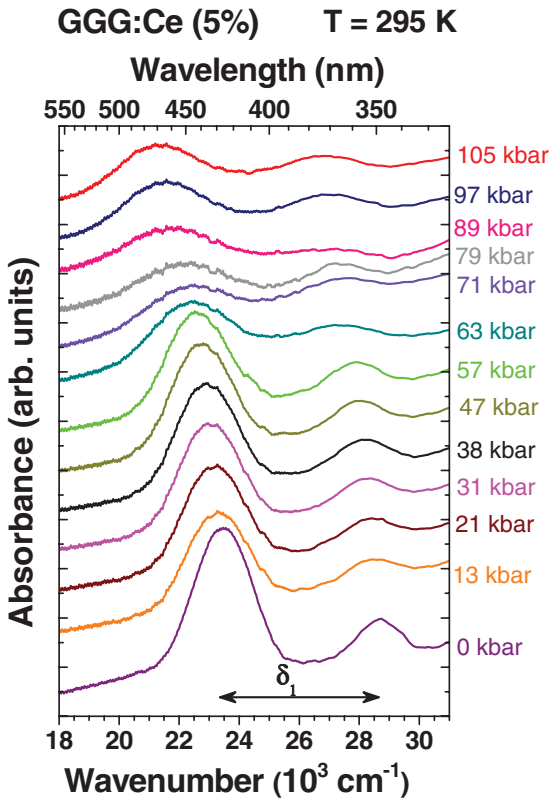

FIG. 5. (Color online) The pressure dependence of the absorption spectra of Ce^{3+} in GGG crystal.

and (1.2 ± 0.9) cm^{-1}/kbar for the crystal field splitting δ_1 parameter, respectively. This last result indicates that the distortion of the Ce^{3+} ion surrounding from perfect cubic structure increases with pressure; however, this increase is very small.

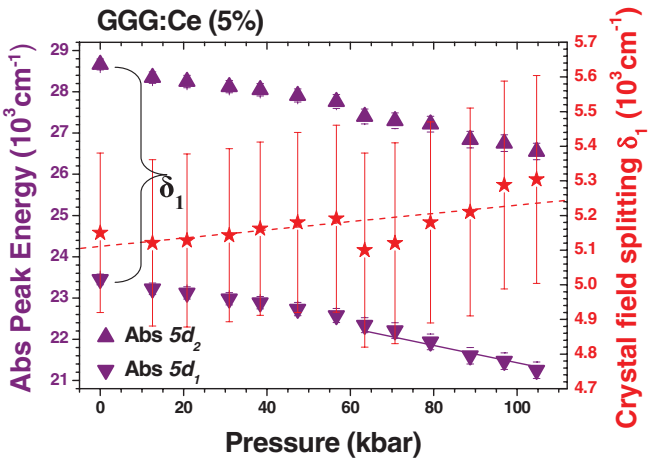

FIG. 6. (Color online) The pressure dependence of the absorption peak energies and the crystal field splitting δ_1 of Ce^{3+} in GGG crystal. The solid line represents the best fit of the model to the experimental data of the $^2F_{5/2} \leftrightarrow 5d_1$ absorption in the region of applicability of the SCC model (see the description in Sec. IV A). The dashed line represents the linear fit to the pressure dependence of the crystal field splitting δ_1.

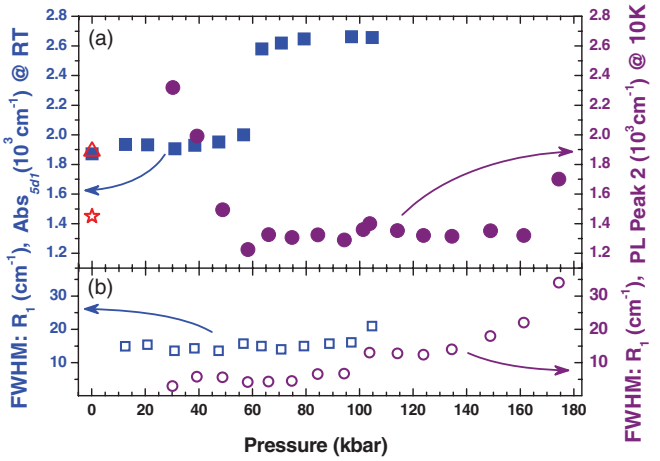

FIG. 7. (Color online) (a) The pressure dependence of absorption (squares) and emission (circles) FWHM for the $^2F_{5/2} \leftrightarrow 5d_1$ transition. Here, PL was measured at 10 K, absorption was measured at RT. The FWHM of ambient-pressure absorption measured on bulk GGG:Ce sample at 10 K and RT is marked by an open star and a triangle, respectively. (b) The pressure dependence of emission FWHM of the ruby R_1 line used as a pressure sensor at absorption (squares, RT) and PL (circles, 10 K) measurements in DAC.

D. Pressure dependence of the spectral bandwidth of Ce^{3+} absorption and photoluminescence in GGG crystal

Before applying a single configuration coordinate (SCC) model for description of the observed phenomena, we have to analyze the spectral bandwidth of both absorption and photoluminescence lines corresponding to the transition between the same electronic states, i.e. to the $^2F_{5/2} \leftrightarrow 5d_1$ transition. In this way, we can check the range of applicability of this model, according to which the mirror symmetry between absorption and emission line shapes is expected, as the electron-phonon coupling is assumed to be the same in the ground and excited states.[62,63]

Figure 7(a) presents comparison of the pressure dependence of absorption and emission full width at half maximum (FWHM) for the $^2F_{5/2} \leftrightarrow 5d_1$ transition. The important aspect, which should be taken into account, is the fact that all PL spectra were measured at 10 K, whereas high-pressure absorption spectra were measured at RT, which contributes to additional increase of absorption bandwidth. The difference between low- and room-temperature absorption spectra can be taken into account by comparing the respective ambient-pressure absorption measured on the bulk GGG:Ce sample. The ambient-pressure FWHM of $^2F_{5/2} \rightarrow 5d_2$ transition at 10 and 295 K is marked in the graph by an open star and a triangle, respectively.

Additionally, in the case of high-pressure measurements in DAC, the FWHM analysis is not straightforward because of possibility of occurrence of nonhydrostaticity effects, which can contribute to the increase in the spectral bandwidth. These effects can be controlled by monitoring the pressure changes of the line width of ruby luminescence, used as a pressure sensor inside the DAC.[50,51] The pressure dependence of emission FWHM of the ruby R_1 line collected at absorption (squares, RT) and PL (circles, 10 K) measurements in DAC is presented in Fig. 7(b).

Taking into account all the above-mentioned effects, it can be seen that absorption bandwidths at pressures from 0 to 60 kbar are comparable to PL bandwidths at pressures from 60 to 170 kbar. The abrupt increase in absorption FWHM above 60 kbar is not clear. One of the possible reasons of this effect can be some problem with hydrostaticity in the DAC, connected with the extremely sophisticated double-gasket measuring technique. In spite of the stable FWHM of the ruby R_1 line in this range of pressure, it could happen that the compressed gasket started to exert some kind of axial stress on the sample, which is much larger than the ruby ball. However, because the abrupt increase in absorption FWHM occurred at the characteristic pressure of 60 kbar, the unambiguous explanation of this strange result needs additional study.

The FWHM of the emission band is determined from the deconvolution of two Gaussian bands (such a procedure is justified in the case of strong electron-lattice coupling),[55,62] corresponding to the transitions from the $5d_1$ excited state to the $^2F_{7/2}$ and $^2F_{5/2}$ sublevels of the $4f$ ground state (see Fig. 2). Additionally, the emission spectra are affected by ruby luminescence; so the results can be burdened by quite large error; however, they still can provide useful information concerning trends in pressure changes of emission bandwidth. Thus, in the pressure range of 30–60 kbar, when the luminescence appears and its intensity grows rapidly, the luminescence line is visibly broader than the respective absorption. At about 60 kbar, the FWHM reaches its minimum and remains approximately constant up to over 160 kbar. The increase in FWHM at 174 kbar is clearly correlated with the increase in FWHM of the R_1 line pointing to the emergence of nonhydrostaticity inside the DAC. Actually, taking into account a small but continuous increase in the R_1 line FWHM with increasing pressures during PL measurements, we cannot exclude that the luminescence FWHM would even decrease if we would be able to maintain strictly hydrostatic Z conditions.

The exceptionally broad photoluminescence between 30 and 60 kbar can be explained by the formation of the anomalous state being a mix between the states from the bottom of the GGG conduction band and the cerium $5d$ state. This mixing is a result of a special energetic position of the $5d$ state relative to the CB bottom, which changes with pressure. The possible arrangement of the involved energetic relationships is presented in Fig. 8. In the case of CTE formation, the initial energetic position of the anomalous state should be located below the bottom of the CB by an amount close to the binding energy of the electron to Ce^{4+}, i.e. by about 0.5–0.7 eV.[38] As on the basis of our results we cannot determine this value and its pressure changes with respect to the CB bottom, we put the energy level of this state just at the CB bottom for simplicity, and this does not influence the further conclusions. Additionally, there are no available data on band-gap pressure coefficients of any garnets, but as GGG belongs to direct band-gap materials[64] and high-pressure studies of other direct band-gap materials have shown that pressure increases the direct gap, we assumed in the scheme the positive pressure coefficient of GGG.

Applying pressure to the GGG:Ce system, we observe different types of processes in three pressure regions in the dependence on the location of the first excited $5d_1$ energy level of Ce^{3+} with respect to the conduction band bottom of the GGG host:

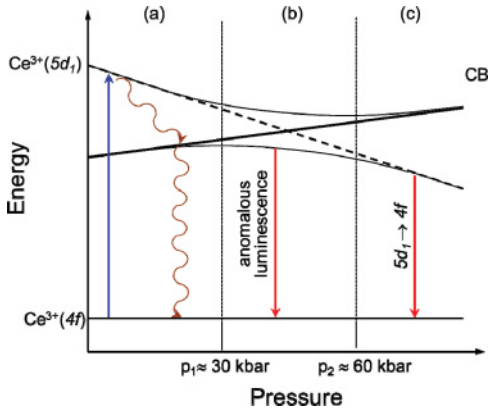

FIG. 8. (Color online) The scheme of pressure-induced changes of energy levels of the Ce^{3+} ion, the conduction band bottom of the GGG crystal, and the mix of the cerium $5d_1$ state with CB states. The pressure boundaries p_1 and p_2 separate the pressure ranges, in which (a) complete luminescence quenching, (b) anomalous luminescence of the mixed state, and (c) Ce^{3+} intraconfigurational $5d_1 \rightarrow 4f$ luminescence is observed. See the text for more detail.

(1) at pressures below 30 kbar, when the emitting $5d_1$ state of Ce^{3+} is resonant with the CB, the complete quenching of radiative emission is observed due to the efficient delocalization of excited electrons and large lattice relaxation around Ce impurity, facilitating effective nonradiative decay through host lattice processes;

(2) at pressures between 30 and 60 kbar, when approaching the energy level crossing, the $5d_1$ state of Ce^{3+} ion is mixed with the states of the CB bottom, which results in appearance of broad and initially weak emission due to the still active nonradiative processes;

(3) at pressures exceeding 60 kbar, when the emitting $5d_1$ state of Ce^{3+} is well below the bottom of the CB, typical highly efficient $4f^05d \rightarrow 4f^1$ emission of Ce^{3+} is observed.

All types of these processes were reported and discussed by many authors in different host crystals doped with Ce^{3+},[25,27,28,56,65] and in more detail in ionic crystals doped with Yb^{2+} and Eu^{2+} ions,[39–45] but they were never observed in one crystal subjected to different pressure conditions only. However, it has been demonstrated that, in Eu^{2+}-doped fluorides, high pressure can transform anomalous luminescence into the conventional $4f^65d \rightarrow 4f^7$ emission.[42–45]

The above analysis shows that the SCC model, assuming the same electron-lattice coupling in the ground and excited states (i.e. one average energy of local phonon modes around Ce^{3+}), can be applied to the highest-pressure region only.

E. Pressure dependence of the Stokes shift between absorption and emission of Ce^{3+} ions in GGG crystal

The pressure measurements of luminescence and absorption spectra of Ce^{3+} dopant in GGG crystal enabled us to determine the pressure dependence of the absorption-emission Stokes shift (Δ_S), defined as the difference between absorption

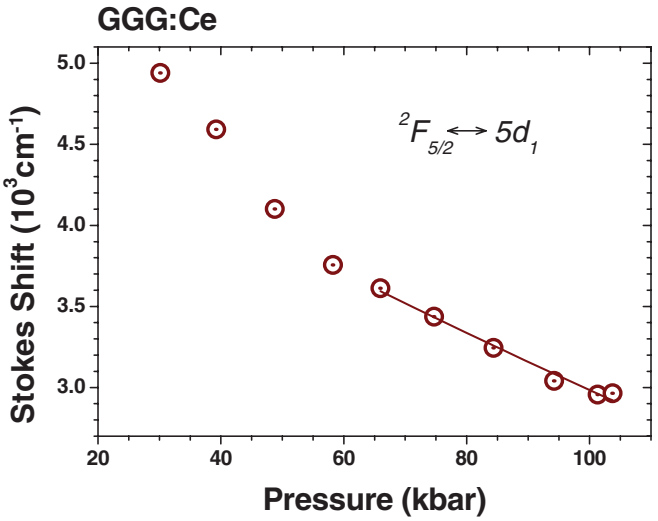

FIG. 9. (Color online) The pressure dependence of the Stokes shift (Δ_S) of the $^2F_{5/2} \leftrightarrow 5d_1$ transition of Ce^{3+} in GGG crystal. The solid line represents the best fit of the model to the experimentally determined Stokes shift dependence of the $^2F_{5/2} \leftrightarrow 5d_1$ transition, in the region of applicability of the SCC model (see the description in Sec. IV A).

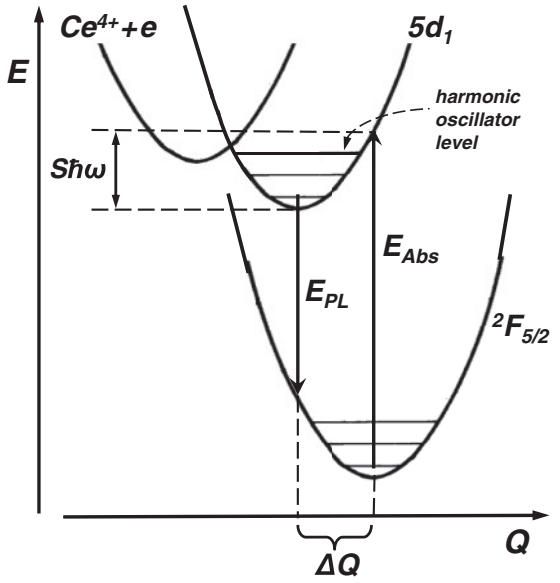

FIG. 10. Configurational coordinate diagram in the harmonic approximation for $p > 60$ kbar, when the CB minimum is shifted over the $5d_1$ emitting energy level. Two parabolas labeled $^2F_{5/2}$ and $5d_1$ represent the ground and excited Ce^{3+} states, and the parabola labeled $Ce^{4+} + e$ corresponds to the Ce^{4+} ion and electron in CB. Harmonic oscillators at the same frequency ω are assumed for both Ce^{3+} states. Here, E_{Abs} and E_{PL} indicated by arrows correspond to the peaks of absorption and emission, respectively.

and emission maximum energies. The pressure dependence of the Stokes shift for the observed transition is shown in Fig. 9.

At pressures between 30 and 60 kbar, where the anomalous emission occurs, a large Stokes shift is observed, which is also one of the fingerprints of such luminescence,[37,38,40–42] as a result of the strong lattice relaxation involved in the photoionization process. It decreases significantly with increasing pressure, which can be associated with the gradual replacement of anomalous luminescence by $5d_1 \rightarrow {}^2F_{5/2}$ transition.

At pressures above 60 kbar, the Stokes shift can be expressed using Huang–Rhys factor S, and $\hbar\omega$—average energy of local phonon modes around Ce^{3+}:[62]

$$\Delta_S = E_{\mathrm{Abs}} - E_{\mathrm{PL}} = (2S-1)\cdot\hbar\omega. \quad (1)$$

The larger Stokes shift (larger Huang–Rhys factor) indicates a stronger electron-lattice coupling and more effective nonradiative transitions via the crossover between the low-vibrational levels of the excited $5d$ state and high-vibrational levels of the ground $4f$ state.[20] It is clearly visible in Fig. 9 that, also in this pressure range, Δ_S still decreases with increasing pressure; however, this decrease is much weaker than at pressures below 60 kbar. Similar effect of pressure-induced reduction in the electron-lattice coupling has been described theoretically by Grinberg *et al.* for a hole-trapped exciton[46] and observed by Grinberg *et al.* in Ce^{3+}-doped $Gd_3Sc_2Al_3O_{12}$ garnet crystal.[56]

IV. THEORETICAL ANALYSIS OF EXPERIMENTAL DATA

A. Theoretical analysis of the data based on the configuration coordinate diagram of the system for pressures >60 kbar

For the analysis of the pressure behavior of absorption, luminescence, and resulting Stokes shift, we use a single configuration coordinate model for pressures exceeding 60 kbar, where this model is applicable.[62,63] The configurational coordinate diagram is schematically shown in Fig. 10. Within this model, we consider two main reasons of pressure-induced decrease of the Stokes shift (see Fig. 9): (i) the decrease of the energy of the $5d_1$ electronic state, and (ii) the pressure changes of the electron-lattice coupling. Taking into account theoretical dependence of single d electron energy levels on a crystal field strength[62,66] as well as the published results of pressure dependencies of $4f^{n-1}5d^1 \rightarrow 4f^n$ transitions of different RE ions[55–57,67,68] and our experimental data (Fig. 6), it is reasonable to assume the linear pressure dependence of the energy of $5d_1$ electronic state, i.e.:

$$E_{5d_1}(p) = E_{5d_1}(0) + k_{5d}\cdot p, \quad (2)$$

where $E_{5d_1}(0)$ and $E_{5d_1}(p)$ are the energies of the minimum of the $5d_1$ electronic state at ambient pressure and the pressure p, respectively, and k_{5d} is the pressure derivative of the $5d_1$ state, which is negative, as the increasing crystal field causes the red shift of this emitting lowest state of the split $5d$ manifold.[62,66,69]

For determination of the type of pressure dependence of the configurational coordinate, we use the relation:[62,69]

$$S(p)\cdot\hbar\omega = \tfrac{1}{2}M\omega^2\cdot[\Delta Q(p)]^2, \quad (3)$$

and resulting directly from this relation dependence:

$$\Delta Q(p) = \sqrt{\frac{2S(p)\cdot\hbar}{M\omega}}, \quad (4)$$

where $S(p)$ is the pressure-dependent Huang–Rhys factor, M is an effective ionic mass, $\Delta Q(p)$ the lateral displacement of the ground and excited state parabolas along configurational coordinate axis (see Fig. 10), and ω the average

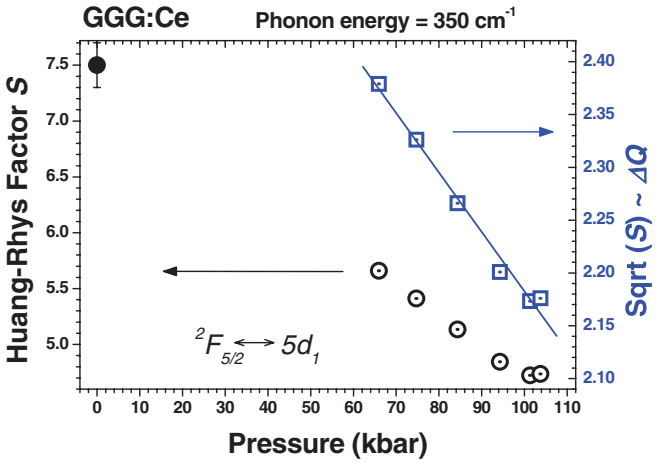

FIG. 11. (Color online) The pressure dependencies of the Huang–Rhys factor (S) of the $^2F_{5/2} \leftrightarrow 5d_1$ transition of Ce^{3+} in GGG crystal, assuming effective phonon energy equal to 350 cm^{-1} (circles) and the square root of the Huang–Rhys factor (squares), proportional to the configurational coordinate (see the text). The linear fit (solid line) to the data is also shown in the graph. The ambient pressure value of the Huang–Rhys factor, determined as $[\Delta Q(0)]^2$, i.e. as the square of the zero point of the configurational coordinate from the linear fit, is marked by the filled circle.

vibrational frequency, assumed to be pressure independent. This assumption is in general not true, as phonon frequencies normally increase slightly with pressure. There is a lack of data concerning pressure coefficients of phonon energies in GGG, but in other RE garnets, these values are in the range of 0.05–0.56 cm^{-1}/kbar,[70–72] and they are small enough to allow such approximation, which considerably simplifies our analysis.

In order to establish the type of the pressure dependence of the configurational coordinate, we need to determine the pressure dependence of the Huang–Rhys factor, which in turn can be obtained using the measured pressure dependence of the Stokes shift from Eq. (1), assuming any reasonable value of the effective phonon energy. We have chosen for such a value the energy of the strongest phonon mode in the Raman spectrum of GGG, equal to about 350 cm^{-1},[73] additionally taking into account the known relation between a Pekarian-shaped bandwidth of the emission and the effective phonon energy and the Huang–Rhys factor:[62]

$$\mathrm{FWHM} = 2.36 \cdot \hbar\omega \cdot \sqrt{S}. \tag{5}$$

According to the discussion of the FWHM of absorption and emission bands from Sec. III D, the results can be burdened by quite large error; however, they still can be used as an indicator of the reasonability of our assumption.

Figure 11 presents the pressure dependence of the Huang–Rhys factor (S) of the $^2F_{5/2} \leftrightarrow 5d_1$ transition of Ce^{3+} in GGG crystal determined from the experimental results of pressure dependence of the Stokes shift (Fig. 9), assuming effective phonon energy equal to 350 cm^{-1}. The obtained values of S decrease from about 5.7 at the pressure of 66 kbar, to about 4.7 at the pressure of 104 kbar.

Figure 11 also shows the pressure dependence of the square root of the Huang–Rhys factor, which according to Eq. (4) is proportional to the configurational coordinate. The results show that the pressure dependence of the configurational coordinate in this pressure range can be described by the linear fit well, which is in the form:

$$\Delta Q(p) = \Delta Q(0) + k_{\Delta Q} \cdot p = \sqrt{\frac{2S(0) \cdot \hbar}{M\omega}} + k_{\Delta Q} \cdot p. \tag{6}$$

Using such a linear pressure dependence of the configurational coordinate and the linear pressure dependence of the energy of the $5d_1$ electronic state [Eq. (2)], we obtained binomial pressure dependencies of the absorption, emission, and the resulting Stokes shift for the $^2F_{5/2} \leftrightarrow 5d_1$ transition:

$$E_{\mathrm{Abs}}(p) = E_{\mathrm{Abs}}(0) + k_{\mathrm{Abs}} \cdot p + k'_{\mathrm{Abs}} \cdot p^2, \tag{7a}$$

$$E_{\mathrm{PL}}(p) = E_{\mathrm{PL}}(0) + k_{\mathrm{PL}} \cdot p + k'_{\mathrm{PL}} \cdot p^2, \tag{7b}$$

$$\Delta_S(p) = \Delta_S(0) + k_{\Delta S} \cdot p + k'_{\Delta S} \cdot p^2, \tag{7c}$$

Then we performed fits to the experimental data for $p >$ 60 kbar. The best fits were parameterized by:

(1) ambient pressure value of absorption energy $E_{\mathrm{Abs}}(0)$, assumed to be equal to (23 500 ± 200) cm^{-1} according to the results of our measurements,

(2) phonon energy $\hbar\varpi$, assumed to be equal to (350 ± 20) cm^{-1},

(3) ambient pressure value of the Huang–Rhys factor $S(0)$, the adjustable parameter,

(4) linear pressure coefficient of the energy of the $5d_1$ state k_{5d} [Eq. (2)], the adjustable parameter,

(5) linear pressure coefficient of the configurational coordinate $k_{\Delta Q}$ [Eq. (6)], the adjustable parameter.

The results of the best fits of this model to the experimental data are presented as solid lines in Figs. 6 and 9. These fits have been obtained for $S(0) = 7.4 \pm 0.2$, and $k_{5d} = (-17 \pm 2)$ cm^{-1}/kbar. The value of the ambient-pressure Huang–Rhys factor obtained from the fit agrees very well with the value of $S(0) = 7.5$ marked in Fig. 9, determined as $[\Delta Q(0)]^2$, i.e. as the square of the zero point of linear fit to the pressure dependence of configurational coordinate ΔQ.

The resulting values of the emission, absorption, and the Stokes shift energies and their pressure dependencies are as follows:

(1) ambient pressure absorption energy $E_{\mathrm{Abs}}(0)$, equal to (23 500 ± 200) cm^{-1}; the pressure coefficients of absorption energy $k_{\mathrm{Abs}} \approx -22$ cm^{-1}/kbar, $k'_{\mathrm{Abs}} = 0.01$ cm^{-1}/$kbar^2$,

(2) presumable ambient pressure emission energy $E_{\mathrm{PL}}(0)$ (although not observed due to non-radiative quenching), equal to (18 700 ± 400) cm^{-1}; the pressure coefficients of emission energy $k_{\mathrm{PL}} \approx -12$ cm^{-1}/kbar, $k'_{\mathrm{PL}} = -0.01$ cm^{-1}/$kbar^2$,

(3) ambient pressure value of the Stokes shift $\Delta_S(0)$ equal to (4800 ± 200) cm^{-1}; the pressure coefficients of the Stokes shift $k_{\Delta S} \approx -10$ cm^{-1}/kbar, $k'_{\Delta S} = 0.02$ cm^{-1}/$kbar^2$.

The obtained agreement between fits and experimental data is very good, and adjusted parameter values are reasonable, which confirms the correctness of our model. This result also shows the relatively high ambient pressure Stokes shift

and Huang–Rhys factor, i.e. strong electron-phonon coupling, which enable nonradiative deexcitation of the $5d$ state.

B. Analysis of the PL energy pressure dependence based on the mixing between the states from the bottom of the GGG conduction band and the Ce^{3+} $5d_1$ state

The pressure dependence of luminescence energy can be modeled taking into account the mixing of the $5d_1$ and CB states, which is expressed quantum mechanically as a superposition of respective wave functions. The degree of mixing depends on the energy separation and the coupling strength between the states. Because of the negative pressure coefficient of the $5d_1$ energy level and positive pressure coefficient of the CB bottom, the energy difference between the $5d_1$ energy level and CB bottom changes with pressure: at ambient pressure, it is positive; then with increasing pressure, decreases to zero causing increase in mixing of states; and afterwards becomes negative (see Fig. 8). Such a situation leads to anticrossing quantum effect.[74] The electronic transitions occur from the lowest mixed state, where the admixture of CB states is the largest at low pressure and decreases with increasing pressure at the expense of the $5d_1$ state. The observed luminescence energy is then equal to:[74]

$$E_{\mathrm{PL}}(p) = E_{5d_1}(0) + \tfrac{1}{2}[p(k_{5d} + k_{CB}) - \Delta E(0) - \sqrt{[\Delta E(0) + p(k_{5d} + k_{\mathrm{CB}})]^2 + 4V^2}], \quad (8)$$

where k_{CB} is the linear pressure coefficient of the CB bottom energy, $\Delta E(0)$ the energy separation between the minimum of the unmixed $5d_1$ energy level and CB bottom, and V the coupling energy between the states.

Using for k_{5d} the value -17 cm^{-1}/kbar obtained from previous fits and for $E_{5d_1}(0)$ the value 20 900 cm^{-1}, equal to $E_{\mathrm{Abs}}(0) - S(0)\hbar\varpi$ (see Fig. 10), we have fitted this model to the experimental pressure dependence of photoluminescence. The best fit, presented as a solid line in Fig. 3, has been obtained for $k_{\mathrm{CB}} = (90 \pm 10)$ cm^{-1}/kbar, $\Delta E(0) = (3200 \pm 300)$ cm^{-1}, and $V = (2000 \pm 200)$ cm^{-1}, which appear to be reasonable values, consistent with the other obtained parameters describing the GGG:Ce system.

V. SUMMARY AND CONCLUSIONS

The study of influence of hydrostatic pressure on the optical properties of Ce impurity in bulk $Gd_3Ga_5O_{12}$ garnet has been presented. Application of pressure to the nonemitting GGG:Ce crystal resulted in the emergence of the luminescence at about 30 kbar and subsequent pronounced increase in the luminescence intensity with increasing pressure. Detailed discussion of the observed effects, taking into account the radiative emission connected with the mixing between the $5d_1$ and CB states at pressures from 30 to 60 kbar and Ce^{3+} $4f^0 5d \rightarrow 4f^1$ emission at pressures above 60 kbar have been presented. A thorough analysis of the pressure behavior of the Ce^{3+} absorption and luminescence above 60 kbar, based on a single configuration coordinate model allowed for determining the values of important spectroscopic parameters characterizing the GGG:Ce^{3+} system and their pressure dependencies.

Our results show that the ambient pressure absence of Ce^{3+} luminescence is caused by the resonant location of the $5d_1$ state in the conduction band of the GGG host crystal when efficient delocalization of excited electron occurs. This process is accompanied by strong host lattice relaxation around the Ce^{4+} impurity, which facilitates effective nonradiative decay of the excited electron to the $4f$ state of Ce. The pressure-induced approach of the CB edge of GGG by the excited $5d$ energy level of the Ce^{3+} increases mixing of band states with the $5d_1$ state, which is revealed by the appearance of radiative emission from this mixed state observed at pressures between 30 and 60 kbar. Then for pressures exceeding 60 kbar, this luminescence is replaced by the pure interconfigurational $5d \rightarrow 4f$ transitions of Ce^{3+} ions. An additional very important factor influencing the luminescence efficiency is the strength of electron-lattice coupling, which is shown to decrease with increasing pressure.

ACKNOWLEDGMENTS

This work was partially supported by the grants of the Polish Ministry of Science and Higher Education during years 2008–2010 (Project No. N N202 203734) and 2010–2012 (Project No. N N202 203838).

*Corresponding author: kaminska@ifpan.edu.pl

[1] S. Kück, Appl. Phys. B : Lasers Opt. **72**, 515 (2001).
[2] A. A. Kaminskii, Laser Photon. Rev. **1**, 93 (2007).
[3] J. M. Robertson, M. W. vanTol, W. H. Smits, and J. P. H. Heynen, Philips J. Res. **36**, 15 (1981).
[4] B. Hüttl, U. Troppenz, K. O. Velthaus, C. R. Ronda, and R. H. Mauch, J. Appl. Phys. **78**, 7282 (1995).
[5] E. Danielson, M. Devenney, D. M. Giaquinta, J. H. Golden, R. C. Haushalter, E. W. McFarland, D. M. Poojary, C. M. Reaves, W. H. Weinberg, and X. D. Wu, Science **279**, 837 (1998).
[6] J. L. Wu, G. Gundiah, and A. K. Cheetham, Chem. Phys. Lett. **441**, 250 (2007).
[7] J. G. Kang, M. K. Kim, and K. B. Kim, Mater. Res. Bull. **43**, 1982 (2008).
[8] Y. P. Fu, S. B. Wen, and C. S. Hsu, J. Alloys Compd. **458**, 318 (2008).
[9] M. Balcerzyk, Z. Gontarz, M. Moszynski, and K. Kapusta, J. Lumin. **87–89**, 963 (2000).
[10] M. Nikl, Meas. Sci. Technol. **17**, R37 (2006).
[11] G. Blasse and A. Bril, J. Chem. Phys. **47**, 5139 (1967).
[12] R. R. Jacobs, W. F. Krupke, and M. J. Weber, Appl. Phys. Lett. **33**, 410 (1978).
[13] D. J. Robbins, B. Cockayne, B. Lent, C. N. Duckworth, and J. L. Glasper, Phys. Rev. B **19**, 1254 (1979).
[14] G. F. Herrmann, J. J. Pearson, and K. A. Wickersheim, J. Appl. Phys. **37**, 1312 (1966).
[15] B. F. Aull and H. P. Jenssen, Phys. Rev. B **34**, 6640 (1986).

[16]J. Andriessen, P. Dorenbos, and C. W. E. van Eijk, Phys. Rev. B **72**, 045129 (2005).
[17]W. W. Holloway Jr and M. Kestigian, Phys. Lett. A **25**, 614 (1967).
[18]P. Y. Jia, J. Lin, X. M. Han, and M. Yu, Thin Solid Films **483**, 122 (2005).
[19]M. E. Doroshenko, M. A. Ivanov, V. B. Sigachev, and M. I. Timoshechkin, Sov. J. Quantum Electron. **22**, 588 (1992).
[20]R. A. Hansel, S. W. Allison, and D. G. Walker, Appl. Phys. Lett. **95**, 114102 (2009).
[21]A. Nakatsuka, A. Yoshiasa, and T. Yamanaka, Acta Cryst. B **55**, 266 (1999).
[22]J. B. Gruber, M. E. Hills, C. A. Morrisom, G. A. Turner, and M. R. Kokta, Phys. Rev. B **37**, 8564 (1988).
[23]U. Happek, J. Choi, and A. M. Srivastava, J. Lumin. **94-95**, 7 (2001).
[24]G. Blasse, W. Schipper, and J. J. Hamelink, Inorg. Chem. Acta **189**, 77 (1991).
[25]W. M. Yen, M. Raukas, S. A. Basun, W. van Schaik, and U. Happek, J. Lumin. **69**, 287 (1996).
[26]W. M. Yen, J. Lumin. **83-84**, 399 (1999).
[27]Y. Shen, D. B. Gatch, U. R. Rodróguez-Mendoza, G. Cunningham, R. S. Meltzer, W. M. Yen, and K. L. Bray, Phys. Rev. B **65**, 212103 (2002).
[28]M. Raukas, S. A. Basun, W. van Schaik, W. M. Yen, and U. Happek, Appl. Phys. Lett. **69**, 3300 (1996).
[29]U. R. Rodriguez-Mendoza, G. Cunningham, Y. Shen, and K. L. Bray, Phys. Rev. B **64**, 195112 (2001).
[30]D. Galanciak, M. Grinberg, W. Gryk, S. Kobyakov, A. Suchocki, G. Boulon, and A. Brenier, J. Phys.: Condens. Matter **17**, 7185 (2005).
[31]A. Kaminska, S. Biernacki, S. Kobyakov, A. Suchocki, G. Boulon, M. O. Ramirez, and L. Bausa, Phys. Rev. B **75**, 174111 (2007).
[32]A. Kamińska, R. Buczko, W. Paszkowicz, H. Przybylinska, E. Werner-Malento, A. Suchocki, M. Brik, A. Durygin, V. Drozd, and S. Saxena, Phys. Rev. B **84**, 075483 (2011).
[33]A. Kamińska, P. Kaczor, A. Durygin, A. Suchocki, and M. Grinberg, Phys. Rev. B **65**, 104106 (2002).
[34]A. Kamińska, J. E. Dmochowski, A. Suchocki, J. Garcia-Sole, F. Jaque, and L. Arizmendi, Phys. Rev. B **60**, 7707 (1999).
[35]M. Ramirez, L. Bausa, S. W. Biernacki, A. Kaminska, A. Suchocki, and M. Grinberg, Phys. Rev. B **72**, 224104 (2005).
[36]P. Dorenbos, E. V. D. van Loef, C. W. E. van Eijk, K. W. Krämer, and H. U. Güdel, Phys. Rev. B **68**, 125108 (2003).
[37]A. Bessiére, P. Dorenbos, C. W. E. van Eijk, L. Pidol, K. W. Krämer, and H. U. Güdel, J. Phys.: Condens. Matter **16**, 1887 (2004).
[38]A. Bessiére, P. Dorenbos, C. W. E. van Eijk, K. W. Krämer, H. U. Güdel, and A. Galtayries, J. Lumin. **117**, 187 (2006).
[39]D. S. McClure and C. Pedrini, Phys. Rev. B **32**, 8465 (1985).
[40]B. Moine, B. Courtois, and C. Pedrini, J. Phys. France **50**, 2105 (1989).
[41]P. Dorenbos, J. Phys.: Condens. Matter **15**, 2645 (2003).
[42]D. B. Gatch, D. M. Boye, Y. R. Shen, M. Grinberg, Y. M. Yen, and R. S. Meltzer, Phys. Rev. B **74**, 195117 (2006).
[43]S. Mahlik, B. Kukliński, Y. M. Yen, R. S. Meltzer, and M. Grinberg, J. Lumin. **128**, 715 (2008).
[44]S. Mahlik, M. Grinberg, L. Shi, and H. J. Seo, J. Phys.: Condens. Matter **21**, 245601 (2009).
[45]S. Mahlik, K. Wiśniewski, M. Grinberg, and R. S. Meltzer, J. Phys.: Condens. Matter **21**, 235603 (2009).
[46]M. Grinberg and S. Mahlik, J. Non-Cryst. Solids **354**, 4163 (2008).
[47]G. J. Piermarini, S. Block, J. D. Barnett, and R. A. Forman, J. Appl. Phys. **46**, 2774 (1975).
[48]H. K. Mao and P. M. Bell, Science **200**, 1145 (1978).
[49]W. B. Holzapfel, J. Appl. Phys. **93**, 1813 (2003).
[50]D. M. Adams, R. Appleby, and S. K. Sharma, J. Phys. E **9**, 1140 (1976).
[51]K. Syassen, High Press. Res. **28**, 75 (2008).
[52]P. Dorenbos, J. Alloys Compd. **341**, 156 (2002).
[53]P. Dorenbos, J. Lumin. **91**, 91 (2000).
[54]P. Dorenbos, J. Lumin. **91**, 155 (2000).
[55]J. Barzowska, M. Grinberg, and T. Tsuboi, Radiat. Eff. Defects Solids **158**, 39 (2003).
[56]M. Grinberg, J. Barzowska, Y. R. Shen, R. S. Meltzer, and K. L. Bray, Phys. Rev. B **69**, 205101 (2004).
[57]M. Grinberg, Opt. Mater. **28**, 26 (2006).
[58]R. Turos-Matysiak, W. Gryk, M. Grinberg, Y. S. Lin, and R. S. Liu, Opt. Mater. **30**, 722 (2008).
[59]A. Kaminska, A. Duzynska, A. Suchocki, and M. Bettinelli, J. Phys.: Condens. Matter **22**, 225902 (2010).
[60]B. R. Jovanić, B. Radenković, and Lj. D. Zeković, J. Phys.: Condens. Matter **8**, 4107 (1996).
[61]C. K. Jayasankar, S. Surendra Babu, P. Babu, W. Sievers, Th. Tröster, and G. Wortmann, J. Phys.: Condens. Matter **16**, 7007 (2004).
[62]B. Henderson and G. F. Imbusch, *Optical Spectroscopy of Inorganic Solids* (Clarendon Press, Oxford, 1989).
[63]C. W. Struck and W. H. Fonger, J. Chem. Phys. **60**, 1988 (1974).
[64]Y.-N. Xu, W. Y. Ching, and B. K. Bricken, Phys. Rev. B **61**, 1817 (2000).
[65]G. Cunningham, Y. Shen, and K. L. Bray, Phys. Rev. B **65**, 024112 (2001).
[66]S. Sugano, Y. Tanabe, and H. Kamimura, *Multiplets of Transition-Metal Ions in Crystals* (Academic Press, New York, London, 1970).
[67]K. L. Bray, Top. Curr. Chem. **213**, 1 (2001).
[68]Yu. Zorenko, V. Gorbenko, M. Grinberg, R. Turos-Matysiak, and B. Kukliński, Radiat. Meas. **42**, 652 (2007).
[69]J. García Solé, L. E. Bausá, and D. Jaque, *An Introduction to the Optical Spectroscopy of Inorganic Solids* (John Wiley & Sons Ltd, West Sussex, England, 2005).
[70]K. Papagelis, J. Arvanitidis, G. Kanellis, S. Ves, and G. A. Kourouklis, J. Phys.: Condens. Matter **14**, 3875 (2002).
[71]J. Arvanitidis, K. Papagelis, D. Christofilos, H. Kimura, G. A. Kourouklis, and S. Ves, Phys. Status Solidi B **241**, 3149 (2004).
[72]R. C. Middleton, D. V. S. Muthu, and M. B. Kruger, Solid State Commun. **148**, 310 (2008).
[73]A. Brenier, A. Suchocki, C. Pedrini, G. Boulon, and C. Madej, Phys. Rev. B **46**, 3219 (1992).
[74]U. Hömmerich and K. L. Bray, Phys. Rev. B **51**, 8595 (1995).